

SCUBA Observations of Dust around Lindroos Stars: Evidence for a Substantial Submillimetre Disc Population

M. C. Wyatt*, W. R. F. Dent and J. S. Greaves

UK Astronomy Technology Centre, Royal Observatory, Blackford Hill, Edinburgh EH9 3HJ

4 March 2003

ABSTRACT

We have observed 22 young stars from the Lindroos sample (Lindroos 1986) at 850 μm with SCUBA on the JCMT to search for evidence of dust discs. Stars in this sample are the less massive companions of B-type primaries and have well defined ages that are 10 – 170 Myr; i.e., they are about to, or have recently arrived on the main sequence. Dust was detected around three of these stars (HD74067, HD112412 and HD99803B). The emission around HD74067 is centrally peaked and is approximately symmetrically distributed out to ~ 70 arcsec from the star. This emission either arises from a two component disc, one circumstellar and the other circumbinary with dust masses of 0.3 and $> 27M_{\oplus}$ respectively, or an unrelated background object. The other two detections we attribute to circumsecondary discs with masses of 0.04 and 0.3 M_{\oplus} ; we were also able to show that a circumprimary disc is present around HD112413 with a similar mass to that around the companion HD112412. Cross-correlation of our sample with the *IRAS* catalogs only showed evidence for dust emission at 25 μm and 60 μm toward one star (HD1438); none of the sub-mm detections were evident in the far-IR data implying that these discs are cold (< 40 K assuming $\beta = 1$). Our sub-mm detections are some of the first of dust discs surrounding evolved stars that were not detected by *IRAS* or *ISO* and imply that 9–14% of stars could harbour previously undetected dust discs that await discovery in unbiased sub-mm surveys. If these discs are protoplanetary remnants, rather than secondary debris discs, dust lifetime arguments show that they must be devoid of small < 0.1 mm grains. Thus it may be possible to determine the origin of these discs from their spectral energy distributions once these have been better defined. The low inferred dust masses for this sample support the picture that protoplanetary dust discs are depleted to the levels of the brightest debris discs ($\sim 1M_{\oplus}$) within 10 Myr, although if the extended emission of HD74067 is associated with the star, this would indicate that $> 10M_{\oplus}$ of circumbinary material can persist until ~ 60 Myr and would also support the theory that T Tauri discs in binary systems are replenished by circumbinary envelopes.

Key words: circumstellar matter – stars: binaries: visual – stars: planetary systems: protoplanetary discs – stars: pre-main-sequence – submillimetre.

1 INTRODUCTION

Most, if not all, stars are born with a disc of gas and dust (e.g., Shu, Adams & Lizano 1987). The fate of such protoplanetary discs is important, since it is within these discs that planets are thought to form through the coagulation of initially sub- μm -sized dust grains (Weidenschilling & Cuzzi 1993; Lissauer 1993). Such grain growth is expected to continue as long as the parent disc remains sufficiently massive and models show that our solar system's terrestrial planets could have achieved a sizeable fraction of their final mass by

this mechanism within 10 Myr (e.g., Lissauer 1993). However, at the same time as grain growth is occurring several other mechanisms are competing to deplete disc material. These mechanisms include: viscous gas drag and Poynting-Robertson light drag, both of which result in the accretion of disc material onto the star; stripping of disc material by a stellar wind and radiation pressure; removal of material during encounters with nearby stars; and photoevaporation, either by the parent star or by an external star (Clarke, Gendrin, & Sotomayor 2001; Hollenbach, Yorke & Johnstone 2000). Clearly the success or otherwise of planet formation depends on whether this process is complete at the time the disc becomes too depleted for planetesimal growth. In this

* Email: wyatt@roe.ac.uk

regard an important observable is how long stars retain their protoplanetary discs.

Observations of the near-IR excess emission from stars in nearby open clusters show that the fraction of stars with detectable discs decreases rapidly with the age of the cluster from around $> 80\%$ for recently formed clusters, down to 0% for 6 Myr-old clusters (Haisch, Lada, & Lada 2001). Similarly no near-IR excess is found in nearby star forming regions for stars older than 3-10 Myr (Strom et al. 1989; Kenyon & Hartmann 1995). However, a near-IR excess only implies the presence of warm dust that resides closer to the star than a few 0.1 AU and it is still possible that massive outer discs exist in the older systems without material in the central AU. The cool outer portions of the discs are best probed using sub-mm/mm observations. Such observations are particularly useful, because they also result in a reliable estimate of the disc mass. This is because the discs are transparent at these wavelengths (so all the mass is observed), and the mass estimates are relatively unaffected by uncertainties in the contribution of the stellar photosphere, as well as being only weakly dependent on estimates of the size of the dust grains and of their emitting temperature (e.g., Zuckerman 2001; see section 6).

However, so far sub-mm/mm studies of the evolution of disc mass in the first 10 Myr have been inconclusive. Such observations show that while the masses of the dust discs (where present) are similar for stars of all spectral types at $30\text{--}70 M_{\oplus}$ (Mannings & Sargent 1997), it is not clear whether this disc mass does (Nürnberg et al. 1997) or does not (Osterloh & Beckwith 1995) decrease with age. The evidence is also inconclusive as to whether the decay of the sub-mm disc is (Skinner, Brown, & Walter 1991; Andre & Montmerle 1994; Duvert et al. 2000) or is not (Beckwith et al. 1990; Osterloh & Beckwith 1995; Nürnberg et al. 1998) coincident with the disappearance of the inner disc. All studies agree, however, that by the time these stars reach the main sequence their protoplanetary discs must have been dispersed. *IRAS* showed that some 15% of main sequence stars harbour dust discs (Lagrange et al. 2000) and the very brightest of these have been detected in the sub-mm (Zuckerman & Becklin 1993; Holland et al. 1998; Greaves et al. 1998; Sylvester et al. 2001; Sheret et al. in preparation). However, these are the only stars > 10 Myr for which discs have been detected in the sub-mm. Also, these discs are both much less massive, typically $< 0.1 M_{\oplus}$ (Holland et al. 1998), than their younger counterparts, and cannot be remnants of the protoplanetary disc, since the lifetime of this material is shorter than the age of the stars (e.g., Backman & Paresce 1993). In fact, these discs must be continually replenished, probably by the collisional break-up of asteroids or comets in the systems (Wyatt & Dent 2002) and are henceforth referred to as debris discs.

Our understanding of how a protoplanetary disc evolves into a debris disc as its host star evolves onto the main sequence has been hindered by the difficulty of finding an unbiased sample of stars of intermediate age. For late-type stars ($< 2M_{\odot}$) it is well-known that few such stars have been identified. Herbig (1978) noted that the T Tauri phase corresponds to just a small fraction of a star's pre-main sequence lifetime and inferred that a significant number of Post T Tauri stars with ages of 10-100 Myr should exist. However, such Post T Tauri stars are notoriously difficult

to find, since they show few signs of youth such as active accretion and are no longer associated with regions of active star formation. The more massive ($> 2M_{\odot}$) counterparts to T Tauri stars, Herbig AeBe stars, on the other hand, are found at all stages of the pre-main sequence and even up to 10 Myr after arrival on the main sequence (Waters & Waelkens 1998). Thus the evolution from protoplanetary to debris disc for higher mass stars might occur after the star arrives on the main sequence.

One method for identifying stars of intermediate age is as the secondaries of binary systems with an O or B type primary (Murphy 1969; Gahm, Ahlin & Lindroos 1983), since in this case the primary must be younger than 150 Myr, and so, assuming coevality, must the secondary. The most comprehensive list of such systems was compiled by Lindroos (1986; hereafter L86) and is comprised of 84 companions in 78 systems. This is often referred to as the *Lindroos sample*. Disc masses have been estimated for several of these Lindroos stars using sub-mm and mm observations (Jewitt 1994; Gahm et al. 1994; Ray et al. 1995). These studies showed no detection of dust around stars older than 10 Myr, thus supporting the hypothesis that protoplanetary discs have been depleted by this time (Jewitt 1994). However, the resulting constraints on dust mass, while below the level of T Tauri and Herbig AeBe discs, did not reach down to debris disc levels. This left open the question of whether protoplanetary discs are rapidly depleted down to, or even below debris disc levels, or whether there is a slow decline of disc mass with age (Jewitt 1994). It was the purpose of the sub-mm observations described in this paper to set limits on the dust around a subset of the Lindroos sample approaching the level of the brightest debris discs.

A description of our subset of the Lindroos sample is given in section 2. The sub-mm observations are described in section 3 and in section 4 we describe the results of these observations. In section 5 this sample is cross-correlated with the *IRAS* database to search for evidence of dust emission in the far-IR. In section 6 we discuss these observations and use them to derive dust masses for this sample and discuss the implications for the evolution of protoplanetary discs. Our conclusions are given in section 7.

2 SAMPLE

The Lindroos sample is comprised of 84 physical companions located 2-60 arcsec from O and B type primaries (L86). These were selected from the Washington Double Star catalogue (Gahm et al. 1983) and then several tests performed to eliminate optical rather than physical associations (Lindroos 1985, hereafter L85). In this manner the sample has already been streamlined from an original list of 290 stars. The ages of the primaries, which are mostly main sequence stars, in all these systems were estimated from Stromgren photometry to be < 150 Myr with half of this sample younger than 30 Myr (L85). Assuming the same age for the secondaries, which have spectral types in the range B2 to K5, 37 of these must still be contracting toward the main sequence with the remainder having recently arrived there (L85).

For our sample we chose stars from table 1 of L86 according to the following criteria. First that they have declinations $\delta > -50^{\circ}$. Second, we chose only those systems with

later ($>B5$) type primaries. This is because the circumsecondary discs in such systems could have been affected by their interaction with the strong stellar wind and high photoionisation flux of the very luminous primary star (e.g., Johnstone, Hollenbach & Bally 1998; O'Dell 2001). We also chose only systems with projected separations > 300 AU. Jensen, Mathieu & Fuller (1996) used sub-mm/mm observations of pre main sequence binaries to show that disc masses are significantly lower for those systems with separations between 1-100 AU, while the disc masses in systems with separations > 100 AU are indistinguishable from those of single stars. This implies that the evolution of protoplanetary discs in systems with intermediate separation are considerably affected by the presence of a companion, presumably because of the truncation of these discs by gravitational perturbations. Our constraints allow us to consider the evolution of the companions and of their discs as being similar to that of single stars independent of the evolution of the primary.

Finally, since the studies of Lindroos and co-authors, the physical association of some of the Lindroos sample has been tested by other authors. One of the methods used was to search for indications of youth in the secondary. Such indications include: high Li abundance (Pallavicini, Pasquini & Randich 1992; Martín, Magazzù & Rebolo 1992), detection of H α or Ca H & K emission (Pallavicini et al. 1992), strong X ray emission (Huélamo et al. 2000; Huélamo et al. 2001), similar space motion to other groups of young stars (Martín et al. 1992). Another method was to check for similarity in the radial velocities of the two components (Martín et al. 1992). In rejecting erroneous Lindroos stars from our sample we took all of these studies into account, in particular omitting all pairs designated as *likely optical* by Pallavicini et al. (1992).

This process left us with 22 stars, which we further split into two categories according to spectral type: a group of 13 young low mass (YLM) stars ($>F0$) comprising Post T Tauri (PTT) and Young Main Sequence (YMS) stars; and another of 9 young high mass (YHM) stars ($<A9$) comprising Post Herbig AeBe (PH AeBe) stars and YMS stars. The characteristics of these stars are shown in Table 1. Of the group of YLM stars, 7 were identified by L85 as still contracting toward the main sequence, while they identified just one of the YHM stars (HD47247B) as not having yet reached the main sequence. The lower fraction of pre-main sequence stars among the higher mass stars in this sample is inevitable given their shorter contraction time relative to the main sequence lifetime of the B-type primaries (L85).

It should be pointed out that the studies described above to test for physical association of the Lindroos sample dealt only with potential members of our low mass group. For this reason we should anticipate that some fraction of our YHM group could in fact be optical pairs (perhaps even up to 50%, Pallavicini et al. 1992). Also, since this list was compiled, a study was published which compared the ages of the two components of 10 of our YLM sample based on their position in the HR diagram relative to evolutionary tracks (Gerbaldi, Faraggiana & Balin 2001). These authors classified three of the stars in our YLM sample (HD90972B, HD108767B and HD127304B) as young, ≤ 100 Myr, a finding corroborated by the detection of X ray emission toward these stars (Huélamo et al. 2000), but not associated with the putative primaries, since the ages they derived for the

three primaries were all 200–240 Myr. Evidently there is still some uncertainty in resolving whether the Lindroos stars are physically associated as well as in determining their ages (see e.g., Hubrig et al. 2001 for another estimate of the ages of 3 of our YLM primaries). In the following discussion we adopted the ages given in L86 where available.

3 OBSERVATIONS

The observations were made using the Submillimetre Common-User Bolometer Array, SCUBA (Holland et al. 1999) at the James Clerk Maxwell telescope (JCMT). Photometry observations were made at 850 μ m wavelength, using the central bolometer on the long-wave array. The locations of the 22 observed (secondary) stars are given in Table 1; the pointing accuracy of the JCMT is estimated to be ± 2 arcsec rms. Two of our sources were observed at 5-6 arcsec from these locations, in one instance because we used coordinates for the secondary taken from SIMBAD rather than calculated from the offset from the location of the primary (HD33802), and the other because of a coordinate transcription error (HD127304). Since the instrumental beam size for these observations is 14.5 arcsec, we would expect to detect the flux from a point source at 60-70% of its peak value; the dust masses derived from the observed fluxes given in Table 2 have been scaled accordingly. Each of our 22 sources was observed for 2 ± 1 hours during observing runs spread out over the period February 2001 to January 2002.

The conventional two position chopping and nodding technique was employed to remove the dominant sky background using a 60 arcsec chop throw in azimuth. The data were corrected for atmospheric extinction using sky opacities that were measured at the JCMT using the skydip method at appropriate intervals throughout the nights (Archibald et al. 2002). The data for each night were calibrated using Mars or Uranus when available, otherwise using the standard secondary JCMT calibrators. The data reduction was accomplished using the SURF package (Jenness & Lightfoot 1998), and anomalous signals were clipped above the 3 σ level.

SCUBA photometry observations also result in data for a further 36 bolometers on the long wave array. The arrangement of these bolometers is such that they cover a ~ 2.3 arcmin diameter field of view, however, they are spaced so that the sky is instantaneously undersampled, thus this data cannot be used to recreate a fully sampled map. The closest of these bolometers is 21 arcsec from the target, corresponding to ~ 600 AU from our most nearby target. Thus we did not expect any circumstellar emission to appear in the remaining bolometers and their data was used to remove sky level variations. However, in section 4.2 we also used these bolometers to test for the presence of more extended emission around these stars. In this instance the bolometers were weighted according to their noise and just the outer ~ 70 arcsec ring of bolometers was used for sky removal.

Table 1. Properties of the Lindroos stars in our sample. Spectral types are taken from L86. Ages are also from L86 except for the one indicated by an asterisk (HD77484); since L86 did not provide an age estimate for this star, its age was taken from Gerbaldi et al. (2001). Distances are from Hipparcos except those (indicated by an asterisk) for which this was not determined with $> 3\sigma$ uncertainty; distances to those stars were taken from L86. Projected separations are from the Washington Double Star catalog (Worley & Douglass 1996), and the location of the secondary (or in one case tertiary) has been calculated using these offsets from the J2000 position of the primary from SIMBAD. The orbital semimajor axes (a in arcsec) of these binary systems have been estimated from their most statistically likely values based on the observed separation (ρ in arcsec): $\log a = \log \rho + 0.13$ (Duquennoy & Mayor 1991). Objects for which excess emission is reported in the current work are shown in bold.

Primary Name	Sp	Age, Myr	Dist, pc	Companion Name	Sp	Sep, "	a , AU	Sep, PA	RA(J2000)	Dec(J2000)
(a) Low Mass Companions										
HD560	B9V	< 50	100	HD560B	G5VE	7.7	1000	160°	00h10m02.38s	+11°08'37.7"
HD1438	B8V	95	212	HD1438B	F3V	6.2	1800	240°	00h18m41.67s	+43°47'25.0"
HD17543	B6IV	62	185	HD17543C	F8V	25.2	6300	110°	02h49m19.21s	+17°27'42.9"
HD27638	B9V	123	82	HD27638B	G2V	19.5	2200	25°	04h22m35.55s	+25°38'03.2"
HD33802	B8V	40	74	HD33802B	G8V	12.7	1300	337°	05h12m17.56s	-11°51'57.5"
HD77484	B9.5V	170(*)	250	HD77484B	G5V	4.8	1600	92°	09h02m50.97s	+00°24'29.3"
HD90972	B9.5V	120	147	HD90972B	F9VE	11.0	2200	226°	10h29m34.77s	-30°36'33.0"
HD108767	B9.5V	< 112	27	HD108767B	K2VE	24.1	880	214°	12h29m50.92s	-16°31'15.6"
HD112413	A0IIIP	< 28	34	HD112412	F0V	19.3	890	228°	12h56m00.45s	+38°18'53.3"
HD127304	A0V	< 79	107	HD127304B	K1V	25.8	3700	256°	14h29m47.71s	+31°47'22.1"
HD129791	B9.5V	45	130	HD129791B	K5V	35.3	6200	206°	14h45m56.20s	-44°52'34.8"
HD143939	B9III	< 32	168	HD143939B	K3V	8.6	1900	217°	16h04m44.04s	-39°26'11.7"
HD145483	B9V	< 71	91	HD145483B	F3V	3.8	470	71°	16h12m16.31s	-28°25'01.1"
(b) High Mass Companions										
HD3369	B5V	56	163(*)	HD3369B	A6V	35.9	7900	173°	00h36m53.20s	+33°42'34.0"
HD35173	B5V	44	331(*)	HD35173B	B7V	26.0	12000	285°	05h23m30.00s	+16°02'32.5"
HD47247	B5V	14	230	HD47247B	A2V	9.1	2800	336°	06h36m40.79s	-22°36'44.7"
HD63065	B9.5V	110	293(*)	HD63065B	A2V	17.4	6900	9°	07h47m02.65s	+00°01'23.3"
HD74067	B9V	63	86	HD74067B	A2V	4.0	460	68°	08h40m19.49s	-40°15'48.4"
HD91590	AP	38	259(*)	HD91590B	AP	28.4	9900	162°	10h33m33.27s	-46°59'00.2"
HD99803	B9Vp	126	100(*)	HD99803B	A3V	13.1	1800	168°	11h28m35.33s	-42°40'39.9"
HD159574	B81b	46	938(*)	HD159574B	B7V	12.9	16000	341°	17h37m19.37s	-40°19'00.2"
HD177817	B8IV	100	224(*)	HD177817B	A0V	6.4	1900	2°	19h06m52.14s	-16°13'39.0"

4 RESULTS OF SCUBA OBSERVATIONS

4.1 Photometry

The results of the observations described in section 2 are given in Table 2. The 1σ uncertainty achieved in these observations is 2 ± 1 mJy, resulting in 3σ upper limits of ~ 5 mJy. This is an order of magnitude improvement over previous observations which were obtained at the JCMT using the instrument UKT14 (Jewitt 1994). Sub-mm emission was detected in the central bolometer toward three stars in our sample at the 3σ level, HD74067B (7.2 ± 1.5 mJy), HD112412 (3.8 ± 1.1 mJy) and HD99803B (4.7 ± 1.6 mJy). Two of these stars are from the high mass group, resulting in a detection rate of 22% for this group, while one of the low mass stars was detected (a detection rate of 8%).

Given the high sensitivity of the observations, we might expect some detections in our sample simply from background sources such as high redshift galaxies falling within our beam. Several estimates have been made of sub-mm number counts, the most recent being the SCUBA 8 mJy survey (Scott et al. 2002). Scott et al. estimate that there are about 620 sources per square degree above 5 mJy at $850\mu\text{m}$; as many as ~ 2000 sources per square degree should be detected above 3 mJy (Eales et al. 2000). Thus we would expect there to be one background source in any given SCUBA field of view (2.3 square arcmin) at the level of > 5 mJy.

However, only one in a hundred of these sources would fall within the central photometry bolometer. Thus the probability of erroneously detecting a 5 mJy source in our sample of 22 sources is about 1 in 5. While there is a small (20 %) chance that one of our detections is in fact of a background source, it is very unlikely that all three sub-mm sources are unassociated with the program stars.

With such a high sensitivity it is also necessary to check whether we might (or indeed should) have detected the photospheric emission of any of the stars. However, even the two closest primaries (HD108767 and HD112413) have predicted photospheric fluxes of < 0.6 mJy at $850\mu\text{m}$. The more distant primaries, as well as all the secondaries, have predicted fluxes much less than this.

Another consideration for our observations given the large beam size is that for several of our sources the primary falls within the beam when pointing at the companion (e.g., if their separation is less than about 7-8 arcsec, see Table 1). In such cases any emission that is detected could originate near the primary and not the secondary star. Consider the HR4796 wide binary system which hosts a circumprimary disc, but not a circumsecondary disc (Jayawardhana et al. 1998). At 7.7 arcsec separation a SCUBA $850\mu\text{m}$ observation centred on the companion would have detected $\sim 46\%$ of the emission from the circumprimary disc (i.e., ~ 9 mJy Greaves, Mannings & Holland 2000). This uncertainty is rel-

Table 2. Properties of the Lindroos stars in our sample both observed and derived in this paper. All fluxes are in mJy. *IRAS* fluxes come directly from the Faint or Point Source Catalogs (FSC and PSC respectively), apart from those indicated by an asterisk which were calculated using SCANPI (see text for details). *IRAS* data has not been colour corrected. Upper limits from the PSC and SCANPI are quoted at the 3σ level, while those from the FSC are at the 90% confidence level. Disc masses only include the dust mass and were calculated using Equation 1; upper limits correspond to the 3σ uncertainty and assume a dust temperature of 30 K, while the range of masses for detected discs correspond to the range of possible disc temperatures (see text and Table 3).

Source	IRAS	F_{12}	F_{25}	F_{60}	F_{100}	F_{850}	Disc mass, M_\oplus
(a) Low Mass Companions							
HD560B	F00074+1051	278 ± 44	< 245	< 130	< 1040	-2.3 ± 1.5	< 0.5
HD1438B	F00160+4330	128 ± 31	206 ± 27	413 ± 62	< 1370	-2.4 ± 1.7	0.05
HD17543C	F02465+1715	269 ± 27	< 137	< 307	< 1090	1.2 ± 1.6	< 1.8
HD27638B	F04195+2530	375 ± 45	< 218	< 208	< 2010	0.4 ± 1.5	< 0.3
HD33802B	F05099-1155	508 ± 30	113 ± 20	< 242	< 2720	-1.2 ± 1.7	< 0.5
HD77484B						1.6 ± 1.1	< 2.3
HD90972B	F10273-3021	252 ± 30	< 85	< 269	< 1660	0.6 ± 1.6	< 1.1
HD108767B	F12272-1614	2560 ± 179	649 ± 71	< 217	< 497	1.0 ± 1.5	< 0.04
HD112412	F12536+3835	2340 ± 140	605 ± 61	110 ± 31 (*)	< 270 (*)	3.8 ± 1.1	$0.02 - 0.06$
HD127304B	F14276+3200	153 ± 23	< 77	< 210	< 379	1.1 ± 1.1	< 0.6
HD129791B						0.5 ± 2.0	< 1.1
HD143939B						-3.3 ± 1.9	< 1.8
HD145483B	F16091-2817	298 ± 36	< 184	< 632	< 2700	-0.6 ± 2.0	< 0.5
(b) High Mass Companions							
HD3369B	F00341+3326	485 ± 34	< 120	< 99	< 577	1.4 ± 1.4	< 1.2
HD35173B						-3.0 ± 1.7	< 6.1
HD47247B	F06345-2234	120 ± 26	< 70	< 120	< 742	-1.5 ± 1.6	< 2.8
HD63065B						-1.1 ± 1.4	< 4.0
HD74067B	P08385-4005	365 ± 40	< 355	< 910 (*)	< 10600 (*)	7.2 ± 1.5	0.3
HD91590B						-0.7 ± 2.3	< 5.1
HD99803B	F11261-4223	402 ± 36	< 117	< 186	< 1370	4.7 ± 1.6	$0.2 - 0.9$
HD159574B						-1.3 ± 2.9	< 84
HD177817B						1.0 ± 1.8	< 3.0

event for our detection of emission toward HD74067B, since this star is just 4 arcsec from HD70467A. If the emission we detected for HD74067B is actually centred on the primary (and point-like), it would have been underestimated in Table 2 by 80%. The emission detected in the vicinity of HD112412 and HD99803B, however, could not have its origin near the primary stars in these systems, since at 19.3 and 13.1 arcsec offset, these lie outside the beam.

4.2 Search for Extended Emission

In general any emission from circumstellar discs in the systems we observed should come from within a few arcsec of the stars assuming these discs have a typical size of less than a few hundred AU, and so should lie within the central bolometer. However, in the case of HD74067 we were inspired to search for emission from the region around this system because it is in the galactic plane (galactic latitude $b = 0.52^\circ$) with extended cirrus emission nearby (though not peaked on this system) evident from the *IRAS* 100 μ m image. It was thus questionable as to whether the detection is of a circumstellar disc, cirrus heated by the stars, or indeed the chance alignment of a background or foreground cirrus hotspot. One test is to see if the emission is extended on greater than arcminute scales, since this is a characteristic of other cirrus hotspots detected both in the far-IR from its thermal emission (Gaustad & Van Buren 1993) and in the optical as reflection nebulosity (Kalas et al. 2002).

Thus we repeated the data reduction using the outer ring of 18 bolometers at 62-82 arcsec from the centre of the array to estimate the sky level. We then looked at the mean flux levels in the rings of 6 and 12 bolometers at 21-28 arcsec and 40-55 arcsec from the centre respectively; this part of the reduction was done in IDL. Significant emission was indeed detected in both rings, decreasing from an average mJy/beam of 6.7 ± 1.4 at the centre¹ to 2.5 ± 0.6 at 25 arcsec and 1.9 ± 0.5 at 47 arcsec from the star. The outer ring at 70 arcsec showed no emission (0.3 ± 0.4 mJy/beam) as expected as this was used to estimate the sky level.

We also checked to see if this emission is symmetrically distributed around the star. To do this we put individual datapoints into different bins according to their radial distance from the star and position angle on the sky and then obtained the mean and standard deviation in each bin with the different bolometers of different observations weighted according to their noise. In this way we split each bolometer ring into four quadrants. The findings are summarised in Figure 1. The emission does appear to be asymmetrical

¹ The average mJy/beam at the centre is a factor of 1.075 lower than the mJy derived by reducing photometry observations (which is the figure given in Table 1), since during such observations the central bolometer performs a 4 square arcsec 9 point jiggle pattern about the centre (Holland et al. 1999). Reduction of photometry accounts for this to find the flux at the centre assuming we are observing a point source.

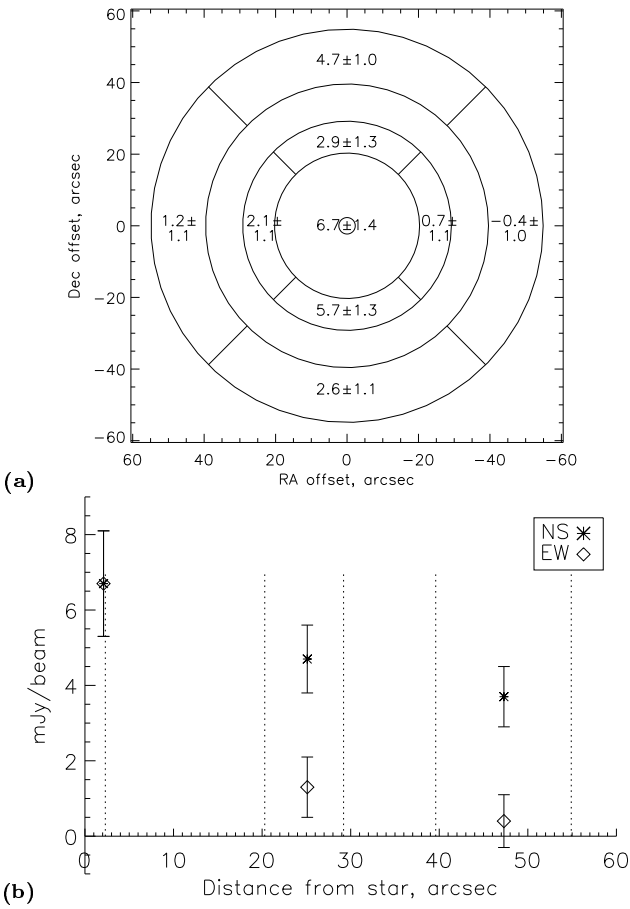


Figure 1. The distribution of the $850\ \mu\text{m}$ emission detected around HD74067B: (a) Undersampled map. The circles show the extent of the first and second rings of bolometers at 21–28 arcsec and 40–55 arcsec respectively. These rings have been subdivided into quadrants and the mean (and its error) of the datapoints falling into each quadrant are shown in units of the average mJy/beam in this region. (b) Radial distribution of emission. Each datapoint corresponds to the average of all data with a position angle within 90° of N or S (asterisk symbol) and E or W (diamond symbol).

in that the only significant emission component is in the N and S directions for both bolometer rings. Combining the data for diametrically opposite quadrants we find that the average mJy/beam in the N+S direction at 25 and 47 arcsec is 4.2 ± 0.9 and 3.7 ± 0.8 respectively, while that in the E+W direction is just 1.3 ± 0.8 and 0.4 ± 0.7 at the same distances. We changed the position angle of the quadrant pattern in Figure 1 to maximise the asymmetry and estimate the error on this angle to be $0 \pm 30^\circ$. An asymmetry is also apparent in the bolometer ring at 70 arcsec, with an average mJy/beam of 1.5 ± 0.6 in the NE+SW direction compared with -1.3 ± 0.6 NW+SE. This indicates that the emission could extend to 70 arcsec from the star. If so, since the mean flux in this bolometer ring was used to subtract the sky emission from the remaining bolometers, the sky level would have been overestimated and the fluxes given in Figure 1 are too low by ~ 1.3 mJy/beam.

While it is possible that the asymmetry is caused by real structure in the emitting material, the signals measured are

also consistent with a symmetrical centrally peaked structure extending to ~ 70 arcsec from the stars. In such an interpretation, the asymmetry arises because some of the symmetrical emission has been artificially eliminated by chopping just 60 arcsec onto the same structure. Because the observations were all undertaken just before or just after transit, the position angle of the azimuth chop was within $\pm 40^\circ$ of E-W for all of our observations. Thus if the emission is centrally peaked, our E+W observations should be lower than those N+S. Assuming the observed N+S emission in Figure 1b is the level at which E+W emission should have been observed if chopping off-source, chopping on-source would have resulted in E+W fluxes ~ 3 mJy/beam lower than those in the N+S direction in both rings of bolometers, consistent with that observed; the emission in the central bolometer would also have been underestimated by a similar amount. To test whether the structure is dependent on chop position angle, we split the dataset into that taken before and after transit, with chop position angles of $72 \pm 7^\circ$ and $126 \pm 6^\circ$ respectively. The position angle of the structure derived was indeed found to be higher for the post-transit observations by $\sim 45^\circ$ for all rings of bolometers. We conclude that this emission extends to 70 arcsec from the star, is centrally peaked and that a significant component is symmetrically distributed around the star.

This process was now repeated for the other stars for which emission was detected. No significant extended emission was detected in the vicinity of either HD99803B or HD1438B. However, additional emission was detected in the bolometer ring 25 arcsec from HD112412 where the average mJy/beam is 2.0 ± 0.4 . Averaging the data points lying within 7.3 arcsec (i.e., within one beam) of different points close to and within this ring showed that this emission can be resolved into three distinct sources (see Figure 2) with no significant emission detected in the remainder of the ring: (i) The first source appears to be centred ~ 4 arcsec N of the primary HD112413 (i.e., at 14 arcsec E and 17 arcsec N of HD112412) with a flux of 5.5 ± 1.6 mJy. Since this source is undersampled, we estimate the uncertainty in its position be ± 5 arcsec and we attribute this emission to a circumprimary disc; this undersampling also means that the absolute level of the emission is not well constrained, with an additional uncertainty estimated to be $\sim 30\%$. (ii) Another source is located 9 arcsec W and 29 arcsec N of HD112412 with a flux of 9.5 ± 1.9 mJy (with similar uncertainties in these values). (iii) A third source is detected almost diametrically opposite HD112413 at a location of 12 arcsec W and 15 arcsec S of HD112412 with a flux of 5.7 ± 1.9 mJy. We note that we would not be able to tell if the emission detected toward HD112412, HD112413 and source (iii) forms part of an extended structure, since the regions between the sources were not sampled (see e.g., Figure 2).

Due to the high proportion of detections we found using this method (2/4), it was questioned whether the non-standard reduction procedure was producing false results. We looked for emission near all the remaining stars in our sample. The only detection was of emission of 7.4 ± 2.1 mJy located 42 arcsec E and 31 arcsec S of HD145483B. In the absence of fully sampled maps it is not possible to determine the true nature of the offset sources (ii) and (iii) near HD112412 and of the source near HD145483B. However as the two additional bolometer rings we checked cover

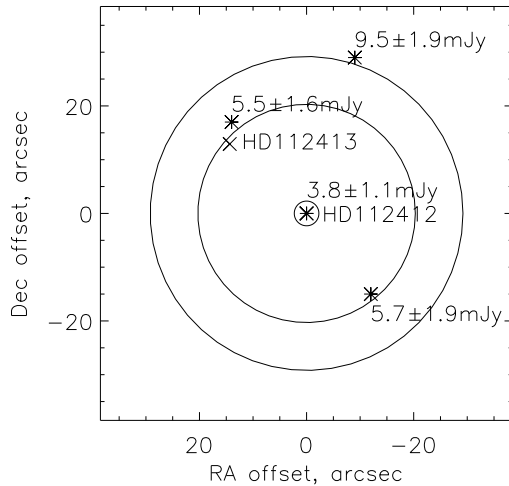


Figure 2. The distribution of the 850 μm emission detected around HD112412. The circles show the extent of the first ring of bolometers at 21–28 arcsec. The circumsecondary disc located at the centre of the map and the three additional sources detected in the first bolometer ring are shown by asterisks and their flux level is also given. The location of HD112413 is shown with a cross.

a ~ 5000 square arcsec field of view, we would expect to detect ~ 5 unrelated background sources in our sample of 22 stars at the ≥ 5 mJy level (see section 4.1), thus we do not discuss these detections further in this paper.

5 CROSS-CORRELATION WITH IRAS

Also shown in Table 2 is a cross-correlation of our sample with the *IRAS* Faint Source and Point Source Catalogs (hereafter FSC and PSC respectively). These catalogs provide flux densities measured in four wavelength bands centred at 12, 25, 60 and 100 μm , and were searched for sources within 60 arcsec of our program stars. In this way emission was detected toward 14/22 of our program stars. Since the FSC is ~ 2.5 times more sensitive than the PSC, these results are shown preferentially. Just one of our detections (HD74067B) did not turn up in the FSC, and this is because the FSC excludes sources within 10° of the galactic plane (i.e., those with $|b| < 10^\circ$).

For all of these detections, the 12 μm flux is consistent with that expected from the photospheres of the primary stars in these systems by extrapolating their K (where available in the literature or from the 2MASS database) or V band magnitudes. The photospheres of the three closest stars (HD108767, HD112413 and HD33802) were also detected at 25 μm . For one of the stars, HD1438, excess emission was detected above photospheric levels at both 25 and 60 μm at 185 ± 31 and 409 ± 62 mJy respectively². The positional uncertainty of the *IRAS* source is such that we cannot distinguish if this emission originates nearer the

² The colour corrected photospheric emission has been subtracted from these fluxes, but no colour correction applied to this excess

primary or secondary component in this system. This uncertainty is particularly pertinent when we consider that a system which just missed inclusion in Lindroos' list because the primary is a main sequence A0 star, HR4796, shows evidence from mid-IR imaging of a dust disc around the primary but not one around the pre-main sequence M-type secondary (Jayawardhana et al. 1998). At 7.7 arcsec separation, it had not previously been possible to tell which star hosted the far-IR emission detected by *IRAS*. We suggest that subsequent mid-IR imaging of this system would resolve this issue.

A similar cross-correlation of the Lindroos sample with the *IRAS* catalogs was performed by Ray et al. (1995) and included 10 of our low mass sample. These authors reported the detection of non-photospheric emission toward 7 of these sources in all four wavebands. It appears that they interpreted all fluxes reported in the *IRAS* catalogs as positive detections, whereas the correct interpretation of a flux reported with FQUAL=1 is that it is an upper limit (3σ for the PSC, 90% confidence for the FSC) as reported in this paper.

Even greater sensitivity can be obtained from the *IRAS* database using SCANPI (*IRAS* Scan Processing and Integration), available at the IRS (Infrared Science Archive) website (<http://irsa.ipac.caltech.edu>). This performs averaging of the *IRAS* raw survey data scans passing close to a given location. We used this to coadd the scans near our survey sources. This resulted in better (3σ) upper limits to the far-IR fluxes at the location of some of our sub-mm detections, as well as the detection of the photosphere of HD112413 at 60 μm . Also, emission was detected centred on HD17543C in the in-scan direction (342° position angle) at 60 μm with a peak of 220 ± 23 mJy. However, this emission appears extended in the cross-scan direction, since a similar level of emission appears in scans taken up to 2 arcmin from the star. Indeed there is a 60 μm only source of 247 ± 42 mJy in the FSC, F02464+1714, located 106 arcsec from HD17543C at a position angle of 254° . We attribute this source either to local cirrus cloud heated by the stars or to an unrelated object and do not discuss it further in this paper.

6 DISCUSSION

6.1 SED Modelling and Dust Masses

While it is clearly unrealistic to model the spectral energy distributions (SEDs) of the infrared excesses of these stars using just one or two datapoints, the upper limits obtained at different wavelengths can set useful constraints on the temperature of the emitting dust. These can then be used to check whether the spatial extent of the emission is consistent with that observed and to compare the sensitivities of the *IRAS* and SCUBA to the types of dust emission that were detected.

The SED is modelled here assuming what is sometimes referred to as *modified black body* emission. The dust is assumed to emit at a single temperature, T , and its emission efficiency Q_ν is assumed to be unity (i.e., to emit like a black body) below a critical wavelength, λ_0 , and to fall off $\propto \lambda^{-\beta}$ at longer wavelengths. Comparison with the observed

and predicted emission properties of real grains shows that $\lambda_0 \approx a$, the typical size of the dust grains, and that β lies in the range 0.5–2 (Bohren & Huffman 1983; Pollack et al. 1994). Interstellar extinction curves show that interstellar-type grains have $\beta \approx 2$ (e.g., Mathis 1990). Modelling of the observed SEDs of young stellar objects (YSOs), T Tauri discs and debris discs around main sequence stars shows that at the early stages of a disc's evolution, $\beta \approx 1.5$ while for more evolved discs $\beta = 0.5 – 1$ (Dent, Matthews, & Ward-Thompson 1998; Dent et al. 2000). Thus, given the age of our sample, we expect their disc emission to be fitted by grains with β close to 1. In the following discussion we set $\beta = 1$ and $\lambda_0 = 100 \mu\text{m}$, and for comparison show also model fits for $\beta = 0$ and 2. The results of the modelling for each star are discussed below (see also Figure 3 and Table 3).

Dust masses were estimated from observed sub-mm flux, since these give a reliable estimate of a disc's dust mass (Zuckerman 2001), although for the far-IR-only detection we used the 60 μm flux. The appropriate formula is (e.g., Zuckerman & Becklin 1993; Zuckerman 2001):

$$M_{\text{dust}} = \frac{F_\nu D^2}{\kappa_\nu B_\nu(T)}, \quad (1)$$

where F_ν is the observed flux, D is the distance to the star, $\kappa_\nu = 0.75Q_\nu/a\rho$ is the dust opacity at the observed wavelength (ρ is the dust density), and B_ν is the black body intensity at the dust temperature. For consistency with the masses derived by other authors (e.g., Zuckerman & Becklin 1993; Holland et al. 1998; Greaves et al. 1998; Sylvester, Dunkin, & Barlow 2001) we adopted a dust opacity of $0.17 \text{ m}^2/\text{kg}$ at 850 μm , and scaled to 60 μm assuming $\beta = 1$ (giving an opacity of $2.4 \text{ m}^2/\text{kg}$). For dust temperatures of 30–100 K, observed fluxes at 850 μm correspond to $11 – 2.7 \times 10^{-3} D^2 F_\nu$ Earth masses, where D is in parsec; dust masses derived from 60 μm fluxes are much more dependent on the assumed temperature of the dust. The derived dust masses for our sample are reported in Table 2.

6.1.1 HD1438B

Since the excess emission is detected at two wavelengths we can derive its temperature to be ~ 107 K. The modified black body fit is shown by the dashed line in Figure 3a. This temperature implies a distance of either 10 AU from HD1438B or 90 AU from HD1438 if the dust emits as a black body. These distances would be larger if the grains are small and so emit hotter than black bodies at an equivalent distance (Wyatt et al. 1999). Thus if this emission is circumprimary, it should be possible to resolve this disc in the mid-IR from an 8 metre class telescope.

It is not surprising that this disc was not detected in the sub-mm, since the fit with $\beta = 1.0$ predicts $F_{850} = 0.8 \text{ mJy}$. In fact our upper limit of 5.1 mJy at 850 μm only rules out that the grains emit as perfect black bodies with $\beta < 0.1$. The upper limit to the dust mass derived from the sub-mm flux is $0.6 M_\oplus$, while the 60 μm flux implies that we have detected material with a mass of just $\sim 0.05 M_\oplus$. This is similar to the mass of the debris discs found around young main sequence stars such as β Pictoris (e.g., Holland et al. 1998). We have also determined the fractional luminosity of the dust disc with respect to that of the star, $f = L_{\text{ir}}/L_*$. If

this is a circumprimary disc $f \approx 0.3 \times 10^{-3}$, a value typical of other debris discs, whereas if circumsecondary $f \approx 0.01$, which would make it one of the most luminous debris discs.

6.1.2 HD74067B

Consider first of all the sub-mm emission detected in the central bolometer. Figure 3b shows fits scaled to the 850 μm flux assuming $\beta = 0.0, 1.0, 2.0$ (dash-dot, dashed and dotted lines respectively). These grain properties and the constraints from the *IRAS* non-detections imply dust temperatures of less than 120, 56, 34 K, and dust masses of at least 0.1, 0.3 and $0.5 M_\oplus$ respectively. It is possible to rule out interstellar-type ($\beta = 2.0$) grains as the origin of this emission, since such grains must lie within 7.3 arcsec of HD74067B and, given the 4 arcsec projected separation of this binary system, are also likely to be within 1000 AU of HD74067. Such grains emit hotter than black bodies since they absorb stellar radiation more efficiently than they re-radiate it at longer wavelengths. The emission efficiencies of interstellar-type grains imply that they would be heated to ~ 110 K at 1000 AU from HD74067 (compared with a black body temperature of ~ 27 K). Since the observed grains are relatively cool for their distance from the primary star (given the *IRAS* limits), we infer that they must have $\beta < 1.0$, although the exact value depends on the assumed value of λ_0 .

While the distribution and level of the emission detected > 25 arcsec from the star remains uncertain due to the nature of our observing method, the fact that this emission was detected implies a substantial mass of dust. If the emission is symmetrically distributed about the stars with a level of 4.2 and 3.7 mJy/beam at 25 and 47 arcsec, this implies integrated fluxes of 45 and 75 mJy in rings of one beam width at these distances. Further assuming emission at black body temperatures (19 and 14 K respectively based on the projected separations from HD74067), this implies dust masses of 7 and $20 M_\oplus$, with more mass expected to have remained unobserved between the bolometer rings.

Similar arguments to those in the paragraph above argue against the presence of interstellar-type grains, since these would be heated to 84 and 66 K at 2200 and 4000 AU from HD74067. However, we note that the interaction of the stars with an interstellar dust cloud would mean that only the largest grains from that cloud could penetrate close to the stars, since the smaller (few $0.1 \mu\text{m}$) grains which dominate the interstellar extinction curves would be repelled by radiation pressure (Artymowicz & Clampin 1997). Thus the cool temperature of the excess emission could not on its own rule out the interaction of the stars with a cirrus cloud as the cause of this excess. However, the mean Galactic density of solid grains is just $\sim 7 \times 10^{-15} M_\oplus/\text{AU}^3$ (Artymowicz & Clampin 1997). Thus, as we infer a mass density from our sub-mm observations of at least $7 \times 10^{-11} M_\oplus/\text{AU}^3$, then if this dust is interstellar in origin, the star must be in a region of the galaxy with at least 10,000 times the mean Galactic density. This is unlikely, since at ~ 60 Myr this system should not still reside in the cloud from which it was born, and such a high density would only apply in molecular clouds which fill just 0.2% of the Galactic stellar disc.

We conclude that the material at > 25 arcsec must be either bound to HD74067 (e.g., in a massive $> 27 M_\oplus$

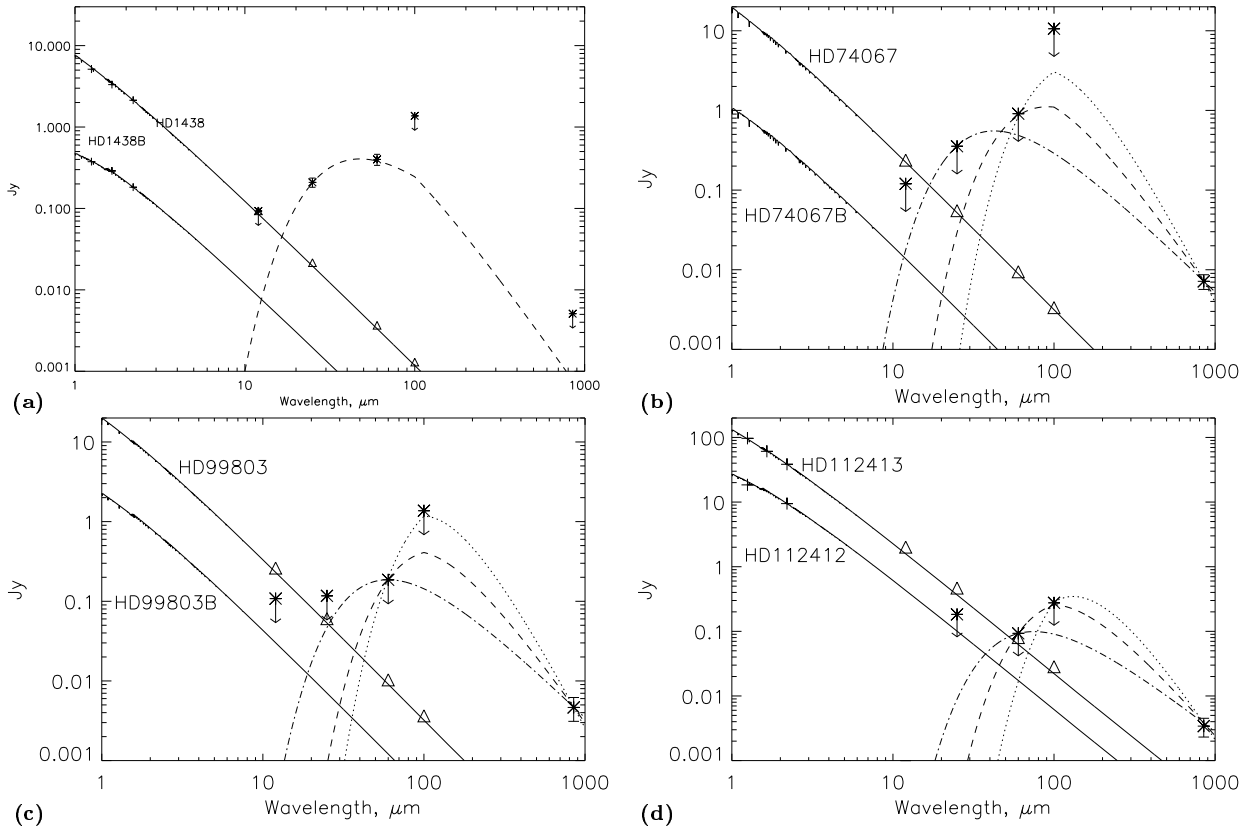


Figure 3. Spectral Energy Distributions of the emission toward the 4 stars for which excess emission is reported in this paper: (a) HD1438B, (b) HD74067B, (c) HD99803B, and (d) HD112412. Stellar spectra were determined from Kurucz model atmospheres appropriate to the spectral type, and were scaled to the K magnitude (or V magnitude if unavailable) which are plotted with plus symbols. The *IRAS* and SCUBA fluxes are plotted with asterisks. Since the *IRAS* fluxes given in Table 2 include a contribution from the photospheric emission of both stars in the system (shown with triangular symbols), this has been colour corrected and subtracted before plotting. In the case of HD1438, the resulting fluxes have been further colour corrected for a 107 K black body. The dashed, dotted and dash-dotted lines show modified black body fits to the excess emission and are discussed in the text; note however that the fits in (b), (c) and (d) are constrained by the textit{IRAS} upper limits and the actual far-IR emission could fall below this level.

Table 3. Results of SED modelling for the emission detected toward HD1438B, HD74067B, HD99803B, HD112412, (see Figure 3). Here we give the derived dust temperature T , the distance from the secondary star r_B of black body grains emitting at this temperature, and the corresponding mass of the M_{dust} for different assumed dust properties defined by the parameter β . The appropriate lines on Figure 3 for these models are also given.

Source	β	T , K	r_B , AU	M_{dust} , M_\oplus	Figure 3
HD1438B	> 0.1	107	10 (or $r_A = 90$ AU)	0.05	dashed
HD74067B	0.0	< 120	> 30	> 0.1	dash-dot
	1.0	< 56	> 130	> 0.3	dashed
	2.0	< 34	> 340	> 0.5	dotted
HD99803B	0.0	< 85	> 50	> 0.2	dash-dot
	1.0	< 42	> 200	> 0.3	dashed
	2.0	< 29	> 420	> 0.5	dotted
	> 20	heating by primary		< 0.9	
HD112412	0.0	< 68	> 40	> 0.02	dash-dot
	1.0	< 38	> 140	> 0.04	dashed
	2.0	< 22	> 410	-	dotted
	> 25	heating by primary		< 0.06	

extended ~ 6000 AU circumbinary disc or remnant protostellar envelope) or an unrelated background object (e.g., a nearby galaxy or Galactic cloud). This system is unusual in our sample for two reasons which argue in favour of the different interpretations: the orbital semimajor axis of this pair (460 AU; Table 1) is the smallest in the sample, thus increasing the chances of survival of a circumbinary disc; and this is the only system in the galactic plane, thus increasing the chance of alignment with a background object. Further observations of this region are required to determine the origin of this emission.

We note that extended circumbinary envelopes have been proposed as the replenishment mechanism of T Tauri discs in binary systems (Prato & Simon 1997), a proposal which may be supported by interferometric observations of binary T Tauri systems which detect a lower level of emission than single dish measurements, possibly implying the presence of additional extended emission (Jensen & Akeson 2003). Also, if this material is circumbinary, then the orbital semimajor axis of the binary (460 AU; Table 1) implies that any circumbinary disc would be truncated within ~ 9 arcsec from a point roughly midway between the two stars (see table 1 of Artymowicz & Lubow 1994). Thus, if this is the case, the emission detected in the central bolometer would have to be circumstellar, not circumbinary, in origin, and further would be truncated at ~ 150 AU (1.7 arcsec) from either star (see table 1 of Papaloizou & Pringle 1977), again ruling out the models with $\beta > 1.0$ (see Table 3).

6.1.3 HD99803B

The SED fit was scaled to the observed 850 μm flux, and upper limits to the temperature of the dust emission calculated for different β . For $\beta = 1.0$, shown with the dashed line in Figure 3c, this temperature must be below 42 K to avoid contradiction with the non-detection by *IRAS*. This corresponds to dust at least 200 AU (2 arcsec) from HD99803B, while the inferred orbital semimajor axis of this system (1800 AU; Table 1) implies that any circumsecondary disc should be truncated beyond 540 AU from HD99803B (Papaloizou & Pringle 1977). This model implies a dust mass of at least $0.3M_{\oplus}$ and a fractional luminosity of 0.6×10^{-3} .

Models with $\beta = 0.0$ and 2.0 are also shown on Figure 3c with dash-dot and dotted lines, respectively. These imply that if the dust emits as a black body, its temperature could be as high as 85 K (dust as close as 50 AU with a mass of $0.2M_{\oplus}$). Interstellar-type dust with $\beta = 2.0$, however, require that $T < 29$ K (dust as close as 420 AU with a mass of $0.5M_{\oplus}$). Dust orbiting HD99803B would be heated to > 20 K by the 1800 AU distant primary star giving an upper limit to the dust mass of $0.9M_{\oplus}$.

6.1.4 HD112412 and HD112413

Starting with HD112412, the SED model was scaled to the observed 850 μm flux, from which upper limits to the temperature of the dust emission were calculated for different β . For $\beta = 1.0$, shown with the dashed line in Figure 3d, this temperature must be below 38 K to avoid contradiction with the non-detection by *IRAS*. This corresponds to dust at least 140 AU (4 arcsec) from HD112412 and implies a

dust mass of at least $0.04M_{\oplus}$ and a fractional luminosity of 4×10^{-5} . Since the emission falls within the beam, we also know that the emission arises < 250 AU from HD112412. This is consistent with the expected truncation radius of the circumsecondary disc due to its tidal interaction with the primary at 260 AU (Papaloizou & Pringle 1977).

Models with $\beta = 0.0$ and 2.0 are also shown on Figure 3d with dash-dot and dotted lines, respectively. These imply that if the dust emits as a black body, its temperature could be as high as 68 K (dust as close as 40 AU with a mass of $0.02M_{\oplus}$). The dust cannot, however, have $\beta = 2.0$, as such models require that $T < 22$ K and so that the dust is further than 410 AU from HD112412; this constraint is incompatible with the emission falling within the beam. In fact both the temperature and distance constraints are also inconsistent with the implied distance to the primary star of 890 AU (Table 1), since this would both truncate the circumsecondary disc (see above) and heat dust falling in the beam centred on HD112412 to > 25 K. This 25 K lower limit to the circumsecondary dust temperature also means that its dust mass is unlikely to be more than $0.06M_{\oplus}$.

Since the *IRAS* upper limits also apply to the emission from the disc around HD112413, and the circumprimary 850 μm emission is the same (within the uncertainty) as that from the circumsecondary disc (see section 4.2), the temperatures and masses derived from the SED models in Figure 3d (see Table 3) are also valid for the circumprimary disc. The factor of ~ 8 times higher luminosity of an A0III to an F0V star, however, means that the limits from these models to the distance of the dust from HD112413 should be approximately 2.8 times the value of r_B given in Table 3. Thus, since for this emission to fall within the beam it must be < 250 AU from the star, we can rule out models with β greater than about 0.5; i.e., to account for the *IRAS* non-detections, the circumprimary grains must emit very much like black bodies at temperatures of < 49 K.

6.2 Detection Summary

Of the 22 stars in our sample, we detected:

- One warm (100–110 K) circumstellar disc toward HD1438 with *IRAS*, but not with SCUBA; it was not possible to tell if this is circumprimary or circumsecondary.
- One system, HD74067, with centrally peaked extended emission, possibly indicating the presence of a nearly face-on circumbinary disc/envelope extending to ~ 6000 AU, and an additional circumstellar component.
- Two cold (< 40 K assuming $\beta = 1$) circumsecondary discs around HD112412 and HD99803B in the sub-mm with SCUBA, but not in the far-IR with *IRAS*; the SCUBA observations also showed that one of these systems hosts a cold (< 50 K assuming $\beta = 0.5$) circumprimary disc (around HD112413).

A quick look at Table 1 shows that, at least within this sample, there is nothing unusual about those systems with circumstellar discs in terms of their age or binarity, since the detected systems span the range of binary separation and age. There does, however, appear to be a correlation with spectral type, since all detections were around stars earlier than F3 ($> 3L_{\odot}$); none of the eight solar-like G or K stars were found to harbour discs. There is also a correlation

with distance in that the two detections in the YHM group were of the closest stars of that group, and that in the YLM group was of the second closest. This leaves the possibility open that all stars in the YHM group and the majority of stars in the YLM group have cold discs that are similar in mass to those detected around HD99803B and HD112412 (see Figure 4).

It is unusual that the circumprimary HD112413 disc is not much more massive than the circumsecondary HD112412 disc, since near-IR and mm observations of binary systems in Taurus-Aurigae show that circumsecondary discs, if present, are much less massive than circumprimary discs (White & Ghez 2001; Jensen & Akeson 2003). A more massive circumprimary disc is also expected from theoretical predictions of binary star formation (Bate & Bonnell 1997), and is certainly true of the quasi-Lindroos system HR4796 (Jayawardhana et al. 1998). However, since HD112413 is the only system in our sample for which information was obtained about its circumprimary emission, we cannot draw any conclusions on this subject.

6.3 Submillimetre Disc Population

What is particularly striking about these results is that 9–14% of this sample (2 or 3 out of 22) have discs that were not detected by *IRAS*. This fraction is even higher at 20–30% (2 or 3 out of 10) if we consider just stars more massive than $1.5M_{\odot}$ ($<F0$), and even higher still (up to 4/11) if we include the the circumprimary disc detected around HD112413. To our knowledge, just one circumstellar disc, that around the M1 star TWA7 (Zuckerman 2001), has been discovered around an isolated star that was not detected first in the far-IR by a space-based telescope such as *IRAS* or *ISO*. The majority of searches for discs in the sub-mm have been directed toward stars for which excess emission is already known in the far-IR. However, such searches are biased toward relatively warm discs. The fact that SCUBA was able to detect these discs while *IRAS* could not must be because these discs are cold (< 40 K if $\beta = 1$; section 6.1). Thus these results imply that a significant population of cold *submillimetre discs* could be awaiting discovery in more unbiased sub-mm surveys, a finding which is supported by the fact that the TWA7 disc was discovered in a sub-mm survey of the TW Hydriæ Association (Zuckerman et al., in preparation), members of which do not necessarily have *IRAS* excesses. Depending on their temperature, these cold discs could also be detected by deep far-IR observations using, e.g., *SIRTF* or *SOFIA*, and indeed such observations in conjunction with those in the sub-mm are required to determine the temperature of these discs³.

Since current estimates put the fraction of main sequence stars with discs at 15% based on the discs that could be detected by *IRAS* (e.g., Plets & Vynckier 1999), an additional cold disc population (i.e., one that *IRAS* could not detect) with the same incidence rate found for our Lindroos sample would mean that the true disc fraction could have

³ Note that until such observations are performed the upper limits to the temperature of this cold disc population are dependent on the assumptions about the shape of the SED, and that a temperature of up to ~ 70 K is possible if $\beta = 0$.

been underestimated by a factor of two. However, it must be remembered that our sample is biased toward young stars. This may be particularly relevant, since TWA7 is also young at ~ 10 Myr (Webb et al. 1999). However, this may be observational bias, since out of the three sub-mm surveys we know about that were undertaken without selection toward stars with *IRAS* excesses (this work; Zuckerman et al., in preparation; Greaves et al., in preparation) two were specifically directed toward young stars.

This does, however, raise the question of whether these discs are (a) debris discs or (b) protoplanetary remnants. The distinction lies in whether these dust discs must be continually replenished from the break-up of a population of large planetesimals. While the transition from protoplanetary to debris disc is likely to be smooth, and there may be no definitive answer, it is important to try to make the distinction because of the implications for the incidence of these discs around older stars. If they can be shown to be protoplanetary remnants they would be much less common around more evolved stars, whereas debris discs could persist over the whole main sequence lifetime of the parent star, albeit getting fainter or less common with age (Habing et al. 1999; Spangler et al. 2001). Also, if they can be shown to be debris discs, it implies that significant grain growth has occurred at large distances from the star.

(a) Planet formation models do predict the existence of cold debris dust rings at large distances from the star (Kenyon & Bromley 2002). In these models a collisional cascade is ignited at a given distance from the star once planetesimals in this region have grown to ~ 1000 km. This makes a bright dust ring which subsequently decreases in brightness until the supply of the 1 km planetesimals that feed the cascade is exhausted. Because of the longer planetesimal growth timescales at larger distances from the star, this means that as the system evolves we would expect to see a bright dust ring expanding out to larger radii until it reaches the edge of the disc. However, this model predicts that cold dust rings at > 150 AU would not occur until a few Gyr. They also do not account for the effect of the binary companion which would stir the planetesimal population making collisions more energetic. This could help the situation by igniting a collisional cascade without having to wait for planetesimals to grow to 1000 km, although this may also hinder it by inhibiting planetesimal growth in the first place.

(b) A different model predicts the existence of cold dust rings left over from the protoplanetary disc (Clarke et al. 2001). This model was developed to explain the rapid removal on a 0.1 Myr timescale of T Tauri discs at an age of ~ 10 Myr, and shows how these timescales can be achieved by the viscous evolution of a gas disc in conjunction with its photoevaporation by the central star. In this model it is just the disc within the gravitational radius (~ 7 AU in their standard model) which is dispersed rapidly (in 0.1 Myr) at 10 Myr; the outer disc is subsequently dispersed over a > 10 Myr timescale as its inner edge expands outwards. Thus Clarke et al. predicted the existence of cold discs that would be preferentially detected in the sub-mm regime beyond ~ 28 Myr, since by this time the only part of the primordial gas disc that would remain would be outside 100 AU. However, a more recent study claims that the rapid clearing of the inner disc is not reproduced when account is

made for the reduction in photoionising flux from the central source when the accretion flux is reduced as the inner disc dissipates (Matsuyama, Johnstone & Hartmann 2003). Rather this study predicts that the outer disc is dispersed at the same rate as the inner disc.

While the models provide conflicting arguments as to the likely origin of the dust, it may be possible to determine this observationally. Dust spirals in toward the central star due to the Poynting-Robertson (P-R) drag force on timescales of $400r^2/\alpha M_\star$ years, where r is the distance of the dust from the star in AU, M_\star is the mass of the star in M_\odot , and the parameter α is the ratio of the radiation pressure force to stellar gravity acting on the dust particles which is a strong function of their size with smaller particles being more affected (e.g., Wyatt et al. 1999). Thus a disc that is 200–540 AU from the 2.3 solar mass star HD99803B would have a P-R drag lifetime for the smallest remnant grains ($\alpha = 1$) of 7–50 Myr. As this is shorter than the age of the system of ~ 120 Myr, for the disc we detected to be primordial (i.e., not second generation), and so for its constituent dust to have survived at this distance from the star over the age of the system, this dust must have $\alpha \ll 0.1$ corresponding to grains much larger than ~ 0.1 mm; i.e., there can be no small (< 0.1 mm) primordial grains in this cold disc.⁴ On the other hand, such small grains are expected to be abundant in a debris disc, since they are continually replenished by the collisional destruction of larger planetesimals that have longer P-R drag lifetimes.

Thus, while we are not proposing that the size distribution of grains in primordial and debris discs should be inherently different, we note that if these discs are protoplanetary, their necessary lack of small (< 0.1 mm) grains would have a potentially discernable effect on their SEDs: if protoplanetary the discs' emission would resemble black body emission with $\beta = 0$ (e.g., Figure 3), whereas if debris discs, their emission would have a β closer to 1. Thus it may be possible to use a shallow sub-mm spectral slope (i.e., emission $\propto 1/\lambda^{2.5}$) to infer a lack of small grains (Dent et al. 1998; Sheret et al. in preparation) and a protoplanetary origin. Further information about grain size could also be derived from SED modelling if the radial location of the dust could be determined by imaging the disc emission (e.g., Wyatt & Dent 2002).

6.4 Evolution of Dust Mass

Leaving aside the uncertainty in the origin of the emission we detected, in Figure 4 we have plotted the dust masses from Table 2 against system age assuming that the emission is circumstellar. This shows how the dust masses derived in this study compare with those of the discs detected around stars of different ages. While the dust mass limits achieved here vary with system distance, for all but the most distant high mass star in our sample we have been able to rule out the presence of dust masses even an order of magnitude below the levels that are characteristic of younger (< 10

⁴ For the $1.6M_\odot$ star HD112412 dust in its disc has a P-R drag lifetime of 5–12 Myr. Similar conclusions to those for the HD99803B disc are less certain due to the uncertainty in the age of this system.

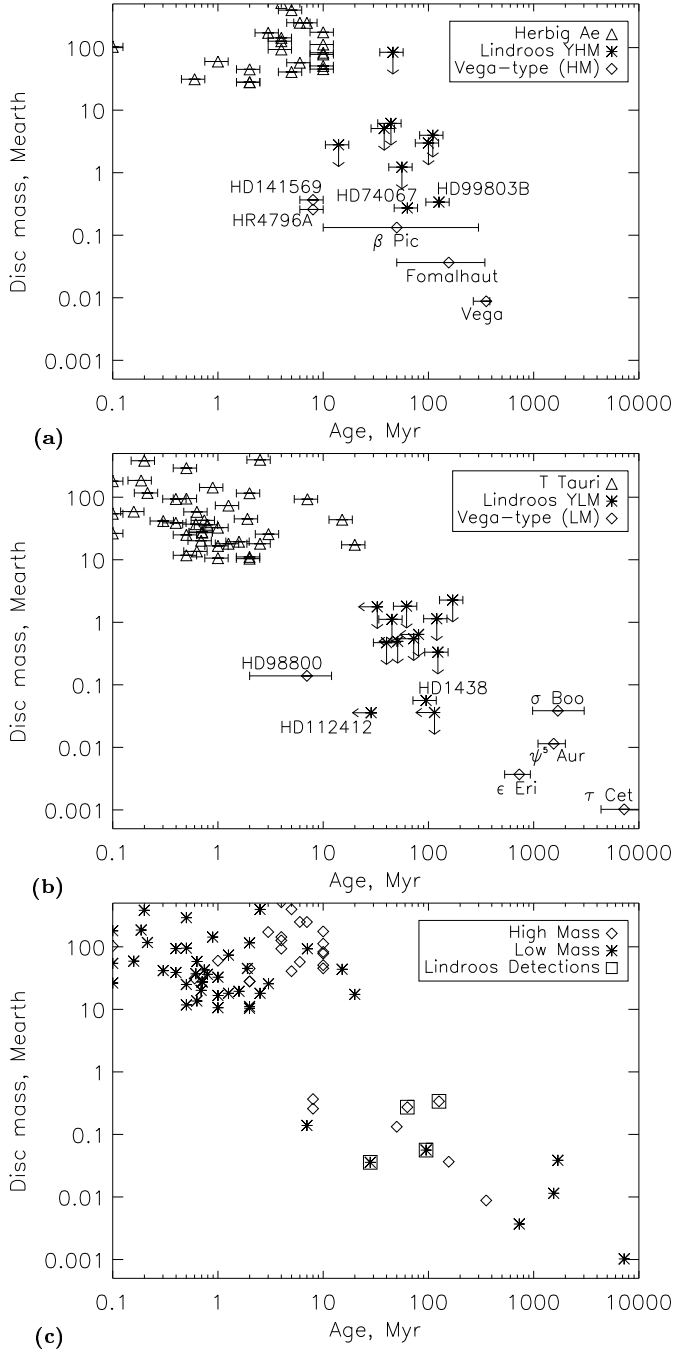


Figure 4. The evolution of dust mass for low mass (a) and high mass (b) stars. For all stars plotted, dust masses were calculated using equation (1) and published sub-mm or mm fluxes as well as estimates of the dust temperature and system distance. As well as the results of this study, we also show detections of T Tauri discs (Jewitt 1994; Osterloh & Beckwith 1995; Nürnberger, Chini & Zinnecker 1997; Nürnberger et al. 1998) and of Herbig AeBe discs (Mannings & Sargent 1997; and lists compiled by Natta et al. 1997 and Meeus et al. 2001); the errors in the ages are nominally plotted at $\pm 25\%$. Also plotted are the Vega-type stars for which sub-mm observations have confirmed the *IRAS* excess to originate in a circumstellar disc (Holland et al. 1998; Greaves et al. 1998; Sylvester et al. 2001; papers by Wyatt, Greaves, Sheret, et al. in preparation), and for which ages, with appropriate errors, are available in the literature (Lachaume et al. 1999; Song et al. 2000; Song et al. 2001). The bottom figure (c) combines the results shown in (a) and (b), and for clarity omits the the Lindroos non-detections and the error in the ages.

Myr) pre-main sequence (T Tauri or Herbig Ae) stars. The dust masses that were detected in this sample, on the other hand, are similar to those of the most massive debris discs. Thus there is no evidence that massive protoplanetary discs persist far beyond ~ 10 Myr.

Figure 4c also emphasizes how protoplanetary and debris discs appear to come from distinct populations, since there are no known discs with masses in the $1\text{--}10 M_{\oplus}$ range. This implies that the evolution from protoplanetary to debris disc occurs rapidly at an age of ~ 10 Myr. However, the apparent gap in the plot could in fact be caused by a combination of the plot strategy and the limited number of disc masses available to be plotted. What Figure 4 really shows is the maximum disc mass that we know exists around stars of different ages. To interpret this correctly we also need to know the fraction of stars at a given age that are plotted in this figure. Studies of young (< 10 Myr) stars are biased toward either classical or weak-line T Tauris (CTTs and WTTs respectively) found in the nearest sites of recent star formation (at ~ 150 pc). The ratio of these populations (WTT/CTT) is uncertain, but could be as high as 10 (Stahler & Walter 1993). The fraction of CTTs and WTTs that have $> 10 M_{\oplus}$ discs is $\sim 50\%$ and $\sim 10\%$ respectively (Osterloh & Beckwith 1995), and the disc fraction for CTTs (but not that of WTTs) may be higher, up to 100%, when this mass limit is decreased to $> 2 M_{\oplus}$ (Duvert et al. 2000). Thus the total fraction of all young (< 10 Myr) stars with massive ($> 2 M_{\oplus}$) discs could be as low as 18% (i.e., $[10\% * 10 + 100\% * 1]/11$). Given that we would expect disc masses for collisionally replenished discs to decline with age $\propto t^{-2}$ as observed (Spangler et al. 2001), we thus might expect that, if this decline starts at ~ 10 Myr, then by 70 Myr (the average age of the Lindroos sample) 18% of stars would have discs more massive than $0.04 M_{\oplus}$. This is consistent with our detection of $\geq 4/22$ discs in the Lindroos sample at this level, and so from this study alone we cannot state that the disc mass decline after 10 Myr must be steeper than t^{-2} .

Rather it is possible that if CTTs and WTTs come from separate populations, and do not form an evolutionary sequence in which CTTs evolve into WTTs in short ~ 0.1 Myr timescales (Skrutskie et al. 1990; Clarke et al. 2001), then a large number of evolved CTTs could have discs with dust masses in the range $1\text{--}10 M_{\oplus}$ and these would be detected once a larger sample of nearby young stars has been observed. Indeed we may already have observed one, since if the emission toward HD74067 is bound to this system, then if this system had been twice as distant (i.e., at a similar distance to the nearest < 10 Myr stars), the larger contribution of the circumbinary material in central bolometer could have resulted in the inference of a $1\text{--}10 M_{\oplus}$ disc. Apart from this Lindroos sample, suitable young (~ 10 Myr) nearby (< 70 pc) candidates include members of the β Pictoris moving group (Zuckerman et al. 2001a) and the TW Hydreae Association (Zuckerman et al. 2001b; Zuckerman et al., in preparation).

7 CONCLUSIONS

Of the 22 young stars in our sample from the Lindroos catalog, we report the detection of sub-mm emission (detected

by us using SCUBA) toward three of these stars and far-IR emission (detected by *IRAS*) toward another star:

- Two of the sub-mm detections (HD112412 and HD99803B) we attribute to cold (< 40 K assuming $\beta = 1$) circumsecondary discs, since these were not detected in the far-IR by *IRAS* and the primary falls outside the beam; these discs have masses of ~ 0.04 and $0.3 M_{\oplus}$, respectively. We were also able to show that a cold (< 50 K assuming $\beta = 0.5$) circumprimary disc is present around HD112413 with a similar mass to the circumsecondary HD112412 disc. These detections imply that current estimates of disc fractions could be underestimated by a factor of two and indicate that a significant cold submillimetre disc population could be awaiting discovery in future sub-mm surveys. It may be possible to determine whether these discs are protoplanetary remnants or debris discs once their far-IR emission and sub-mm spectral slopes have been measured, since the emission, if protoplanetary, would more closely resemble black body emission.

- The sub-mm emission detected toward the third binary system (HD74067) appears to be centrally peaked and extends out to ~ 70 arcsec from the system. The low temperature and high density of this emission means that it is unlikely to be caused by local cirrus heated by the star. Thus this is either a system containing a cold $0.3 M_{\oplus}$ circumstellar disc as well as a $> 27 M_{\oplus}$ circumbinary disc/envelope extending out to ~ 6000 AU, or this is a chance alignment with an unrelated background object. The former interpretation would support the idea that T Tauri discs in binary systems are replenished by extended circumbinary envelopes (Prato & Simon 1997). Since we were chopping onto an extended source, it was difficult to determine the true structure of this emission, thus further mapping of this region will help determine its origin. If this emission is bound to the star this would be an extremely unusual system in that it retains a dust mass of $\gg 1 M_{\oplus}$ until an age of ~ 60 Myr.

- The far-IR emission detected toward HD1438 implies that one of the stars in this system harbours a 107 K, $0.05 M_{\oplus}$ circumstellar disc. If circumprimary, this disc could be resolved with mid-IR imaging from an 8 metre telescope.

The low inferred dust masses for this sample supports the picture that protoplanetary dust discs are depleted to the levels of the brightest debris discs ($\sim 1 M_{\oplus}$) at the end of 10 Myr. However, a larger sample of young stars must be observed before anything more concrete can be said on this subject.

ACKNOWLEDGMENTS

The JCMT is operated by the Joint Astronomy Centre, on behalf of the UK Particle Physics and Astronomy Research Council, the Netherlands Organization for Pure Research, and the National Research Council of Canada. This research has made use of the NASA/ IPAC Infrared Science Archive, which is operated by the Jet Propulsion Laboratory, California Institute of Technology, under contract with the National Aeronautics and Space Administration. We would also like to thank an anonymous referee for helpful comments.

REFERENCES

- Andre P., Montmerle T., 1994, *ApJ*, 420, 837
 Archibald E. N., et al., 2002, *MNRAS*, 336, 1
 Artymowicz P., Lubow S. H., 1994, *ApJ*, 421, 651
 Artymowicz P., Clampin M., 1997, *ApJ*, 490, 863
 Backman D. E., Paresce F., 1993, in Levy E. H., Lunine J. I., eds., *Protostars and Planets III*. Univ. of Arizona Press, Tucson, p. 1253
 Bate M. R., Bonnell I. A., 1997, *MNRAS*, 285, 33
 Beckwith S. V. W., Sargent A. I., Chini R. S., Guesten R., 1990, *AJ*, 99, 924
 Bohren C. F., Huffman D. R., 1983, *Absorption and Scattering of Light by Small Particles*. Wiley, New York
 Clarke C. J., Gendrin A., Sotomayor M., 2001, *MNRAS*, 328, 485
 Dent W. R. F., Matthews H. M., Ward-Thompson D., 1998, *MNRAS*, 301, 1049
 Dent W. R. F., Walker H. J., Holland W. S., Greaves J. S., 2000, *MNRAS*, 314, 702
 Duquennoy A., Mayor M., 1991, *A&A*, 248, 485
 Duvert G., Guilloteau S., Ménard F., Simon M., Dutrey A., 2000, *A&A*, 355, 165
 Eales S., Lilly S., Webb T., Dunne L., Gear W., Clements D., Yun M., 2000, *AJ*, 120, 2244
 Gahm G. F., Ahlin P., Lindroos K. P., 1983, *A&AS*, 51, 143
 Gahm G. F., Zinnecker H., Pallavicini R., Pasquini L., 1994, *A&A*, 282, 123
 Gaustad J. E., Van Buren D., 1993, *PASP*, 105, 1127
 Gerbaldi M., Faraggiana R., Balin N., 2001, *A&A*, 379, 162
 Greaves J. S., et al., 1998, *ApJ*, 506, L133
 Greaves J. S., Mannings V., Holland W. S., 2000, *Icarus*, 143, 155
 Habing H. J., et al., 1999, *Nature*, 401, 456
 Haisch K. E., Lada E. A., Lada C. J., 2001, *ApJ*, 553, L153
 Herbig G. H., 1978, in Mirzoyan L. V., ed., *Problems of Physics and Evolution of the Universe*. Armenian Acad. Sci., Yerevan, p. 171
 Holland W. S., et al., 1998, *Nature*, 392, 788
 Holland W. S., et al., 1999, *MNRAS*, 303, 659
 Hollenbach D., Yorke H. W., Johnstone D., 2000, in Mannings V., Boss A. P., Russell S. S., eds., *Protostars & Planets IV*. Univ. Arizona Press, Tucson, p. 401
 Huélamo N., Brandner W., Brown A. G. A., Neuhauser R., Zinnecker H., 2001, *A&A*, 373, 657
 Huélamo N., Neuhauser R., Stelzer B., Supper R., Zinnecker H., 2000, *A&A*, 359, 227
 Jenness T., Lightfoot J. F., 1998, in Albrecht R., Hook R. N., Bushouse H. A., eds., *ASP Conf. Ser. Vol. 145, Astronomical Analysis Software and Systems VII*. Astron. Soc. Pac., San Francisco, p. 216
 Jensen E. L. N., Akeson R. L., 2003, *ApJ*, 584, 875
 Jensen E. L. N., Mathieu R. D., Fuller G. A., 1996, *ApJ*, 458, 312
 Jewitt D. C., 1994, *AJ*, 108, 661
 Johnstone D., Hollenbach D., Bally J., 1998, 499, 758
 Kalas P., Graham J. R., Beckwith S. V. W., Jewitt D. C., Lloyd J. P., 2002, *ApJ*, 567, 999
 Kenyon S. J., Hartmann L., 1995, *ApJS*, 101, 117
 Lachaume R., Dominik C., Lanz T., Habing H. J., 1999, *A&A*, 348, 897
 Lagrange A.-M., Backman D. E., Artymowicz P., 2000, in Mannings V., Boss A. P., Russell S. S., eds., *Protostars & Planets IV*. Univ. Arizona Press, Tucson, p. 639
 Lindroos K. P., 1985, *A&AS*, 60, 183
 Lindroos K. P., 1986, *A&A*, 156, 223
 Lissauer J. J., 1993, *ARA&A*, 31, 129
 Mannings V., Sargent A. I., 1997, *ApJ*, 490, 792
 Martín E. L., 1997, *A&A*, 321, 492
 Martín E. L., Magazzù A., Rebolo R., 1992, *A&A*, 257, 186
 Matsuyama I., Johnstone D., Hartmann L., 2003, *ApJ*, 582, 893
 Meeus G., Waters L. B. F. M., Bouwman J., van den Ancker M. E., Waelkens C., Malfait K., 2001, *A&A*, 365, 476
 Murphy R. E., 1969, *AJ*, 74, 1082
 Natta A., Grinin V. P., Mannings V., Ungerechts H., 1997, *ApJ*, 491, 885
 Nürnberger D., Chini R., Zinnecker H., 1997, *A&A*, 324, 1036
 Nürnberger D., Brandner W., Yorke H. W., Zinnecker H., 1998, *A&A*, 330, 549
 O'Dell C. R., 2001, *ARA&A*, 39, 99
 Osterloh M., Beckwith S. V. W., 1995, *ApJ*, 439, 288
 Pallavicini R., Pasquini L., Randich S., 1992, *A&A*, 261, 245
 Papaloizou J., Pringle J. E., 1977, *MNRAS*, 181, 441
 Pollack J. B., Hollenbach D., Beckwith S., Simonelli D. P., Roush T., Fong W., 1994, *ApJ*, 421, 615
 Prato L., Simon M., 1997, *ApJ*, 474, 455
 Ray T. P., Sargent A. I., Beckwith S. V. W., Koresko C., Kelly P., 1995, 440, L89
 Scott S. E. et al., 2002, *MNRAS*, 331, 817
 Shu, F. H., Adams, F. C., & Lizano, S. 1987, *ARA&A*, 25, 23
 Skinner S. L., Brown A., Walter F. M., 1991, *AJ*, 102, 1742
 Skrutskie M. F., Dutkiewicz D., Strom S. E., Edwards S., Strom K. M., Shure M. A., 1990, *AJ*, 99, 1187
 Song I., Caillault J.-P., Barrado Y Navascués D., Stauffer J. R., Randich S., 2000, *ApJ*, 532, L41
 Song I., Caillault J.-P., Barrado Y Navascués D., Stauffer J. R., 2001, *ApJ*, 546, 352
 Spangler C., Sargent A. I., Silverstone M. D., Becklin E. E., Zuckerman B., 2001, *ApJ*, 555, 932
 Stahler S. W., Walter F. M., 1993, in Levy E. H., Lunine J. I., eds., *Protostars and Planets III*. Univ. of Arizona Press, Tucson, p. 405
 Strom K. M., Strom S. E., Edwards S., Cabrit S., Skrutskie M. F., 1989, *AJ*, 97, 1451
 Sylvester R. J., Dunkin S. K., Barlow M. J., 2001, *MNRAS*, 327, 133
 Takeuchi T., Artymowicz P., 2001, *ApJ*, 557, 990
 Waters L. B. F. M., Waelkens C., 1998, *ARA&A*, 36, 233
 Webb R. A., Zuckerman B., Platais I., Patience J., White R. J., Schwartz M. J., McCarthy C., 1999, *ApJ*, 512, L63
 Weidenschilling S. J., Cuzzi J. N. 1993, in Levy E. H., Lunine J. I., eds., *Protostars & Planets III*. Univ. Arizona Press, Tucson, p. 1031
 White R. J., Ghez A. M., 2001, *ApJ*, 556, 265
 Worley C. E., Douglass G. G., 1996, *A&AS*, 125, 523
 Wyatt M. C., Dent W. R. F., 2002, *MNRAS*, 334, 589
 Wyatt M. C., Dermott S. F., Telesco C. M., Fisher R. S., Grogan K., Holmes E. K., Piña R. K., 1999, *ApJ*, 527, 918
 Zuckerman B., 2001, *ARA&A*, 39, 549
 Zuckerman B., Becklin E. E., 1993, *ApJ*, 414, 793
 Zuckerman B., Song I., Bessell M. S., Webb R. A., 2001a, *ApJ*, 562, L87
 Zuckerman B., Webb R. A., Schwartz M., Becklin E. E., 2001b, *ApJ*, 549, L233